

Structural and optical properties of $\text{Sb}_{65}\text{Se}_{35-x}\text{Ge}_x$ thin films

S A Saleh^{1,2}, A Al-Hajry¹ and H M Ali^{2,3}

¹ Physics Department, College of Science and Arts, Najran University, PO Box 1988, Najran, Saudi Arabia

² Physics Department, Faculty of Science, Sohag University, Sohag 82524, Egypt

³ Physics Department, College of Science, Al-Baha University, PO Box 1034, 65431 Al-Baha, Saudi Arabia

E-mail: saleh2010_ahmed@yahoo.com and hazem95@yahoo.com (S A Saleh and H M Ali)

Received 7 February 2011

Accepted for publication 18 May 2011

Published 13 June 2011

Online at stacks.iop.org/PhysScr/84/015604

Abstract

$\text{Sb}_{65}\text{Se}_{35-x}\text{Ge}_x$ ($x = 0\text{--}20$ at.%) thin films, prepared by the electron beam evaporation technique on ultrasonically cleaned glass substrates at 300 K, were investigated. The amorphous structure of the thin films was confirmed by x-ray diffraction analysis. The structure was deduced from the Raman spectra measured for all germanium contents in the Sb–Se–Ge matrix. The absorption coefficient (α) of the films was determined by optical transmission measurements. The compositional dependence of the optical band gap is discussed in light of topological and chemical ordered network models.

PACS numbers: 68.55.Ln, 61.50.Ks, 68.55.Jk

(Some figures in this article are in colour only in the electronic version.)

1. Introduction

Chalcogenide glasses are an important class of amorphous materials with various applications, including optoelectronics, integrated optics, electrophotography, solar cells and electrical and optical memory devices. Recently, these materials were applied in rewritable optical data recording (phase change recording). This technology is based on reversible phase transition between crystalline and amorphous states. Currently, the primary materials for phase change recording are based on Sb–Te glasses [1–9], but materials research continues owing to the need of increased storage capacity and data-recording rates. Nowadays, attention is extended to the Sb–Se system as a possible candidate for these applications. Recently, we synthesized ternary Sb–Se–Ge glasses and considered the basic optical parameters depending on glass composition [10]. However, normally the eutectic Sb–Se material system has poor stability, which necessitates the improvement of stability by doping with other elements such as Ge. The higher coordination number of Ge is considered effective in forming covalent bonds and reducing atomic diffusivity, which can provide sufficient amorphous stability; that is, the addition of the third element will create compositional and configurational disorder in the

material with respect to the binary alloy, which will be useful in understanding the structural properties of these materials [11]. Therefore, structural studies of a eutectic SbSe alloy doped with Ge using systematic compositional variation can be useful in gaining important insights into the structure–property relationships of these compounds.

However, several reviews have appeared on the structural, optical and photophysical properties of chalcogenide glasses, which have been the subject of permanent systematic studies for more than 30 years, but on the applications of chalcogenide glasses ([12, 13]; [14] and references therein; [15]), there is no thorough study in the literature on the local atomic structure and its modification in the case of eutectic SbSe alloy doped with Ge. Different experimental techniques such as x-ray diffraction (XRD), scanning electron microscopy (SEM) and Raman spectroscopy are used to study the structure of chalcogenide glasses. Raman scattering is a very powerful experimental technique for obtaining information on the constituent structural units of a given material [16].

The present study aims to investigate the structural and optical properties of the ternary $\text{Sb}_{65}\text{Se}_{35-x}\text{Ge}_x$ system with $x = 0, 5, 10, 15$ and 20 at.% in thin film form.

2. Experimental details

The bulk glassy material of the $\text{Sb}_{65}\text{Se}_{35-x}\text{Ge}_x$ system with $x = 0, 5, 10, 15$ and 20 at.% was prepared from high-purity elements using the conventional melt-quenching technique. Appropriate atomic percentages of high-purity elements (5 N) are vacuum sealed (10^{-5} torr) into fused silica tubes. The sealed tubes are then heated in an electric furnace up to 850°C for 5 h. After complete melting and homogenization, the tubes are quenched in an ice–water mixture. Thin films of the present composition were obtained by electron beam evaporation of bulk in a vacuum of 6.7×10^{-4} Pa and subsequent condensation on an ultrasonically cleaned glass substrate kept at 300 K by using an Edward high-vacuum coating unit (model E306A). The deposition parameters were kept constant for all the investigated films. The film thickness was measured by a digital thickness monitor (Maxtek TM200). The thickness of the films was approximately 200 nm. The films were checked by the energy dispersive spectroscopy (EDS) technique using a field emission scanning electron microscope (Joel JSM 7600F). The amorphicity of the films was confirmed by XRD carried out with a PANalytical (X'pert Pro MPR) in a 2θ scan using $\text{Cu K}\alpha$. Raman spectra of the films were recorded at room temperature with a PerkinElmer (Raman station 400) Raman spectrometer in the wavenumber region $500\text{--}80\text{ cm}^{-1}$ at 4 cm^{-1} resolution, and excitation wavelengths were provided by an Ar⁺ Spectra–Physics laser with an excitation wavelength of 514.5 nm. This wavelength was chosen to avoid any possible photostructural modification that could be induced by the probe beam during measurements. The spectral distribution of the transmittance T and the reflectance R for films was measured at room temperature using unpolarized light at normal incidence in the wavelength range $400\text{--}2500\text{ nm}$ with a dual beam spectrophotometer (JASCO, V-570).

3. Results and discussion

The structure or the structural units of $\text{Sb}_{65}\text{Se}_{35-x}\text{Ge}_x$ were investigated by XRD and Raman spectroscopy. The XRD study confirmed that all films were amorphous with germanium content in the range of Ge concentration $0\text{--}20$ at.% (figure 1). It is seen that all the samples are in the amorphous state where no characteristic crystalline peaks can be observed. The amorphous state was expected for the evaporated films since the quenching rate during the deposition process is much higher than that of the melt–quench alloys [17].

The Raman study provides valuable information on the structural modification through a systematic substitution of germanium. The vibrational bands reported in the literature for their crystalline accompaniment were taken as the reference to discuss the spectrum [18–25]. The Raman spectra of $\text{Sb}_{65}\text{Se}_{35-x}\text{Ge}_x$ ($0 \leq x \leq 20$ at.%) thin films are shown in figure 2. The spectrum of $\text{Sb}_{65}\text{Se}_{35}$ films (with no germanium substitution) exhibits three broad bands located around $88\text{--}120$, $130\text{--}180$ (see inset (A)) and $186\text{--}250\text{ cm}^{-1}$, respectively. The first two bands are assigned to symmetrical pyramidal SbSe_3 bending modes. The weak band positioned at 190 cm^{-1} has been related to homopolar Sb–Sb in

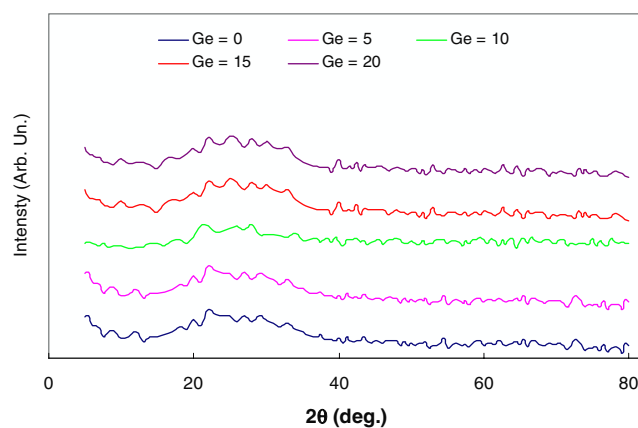


Figure 1. XRD patterns of $\text{Sb}_{65}\text{Se}_{35-x}\text{Ge}_x$ ($0 \leq x \leq 20$) films.

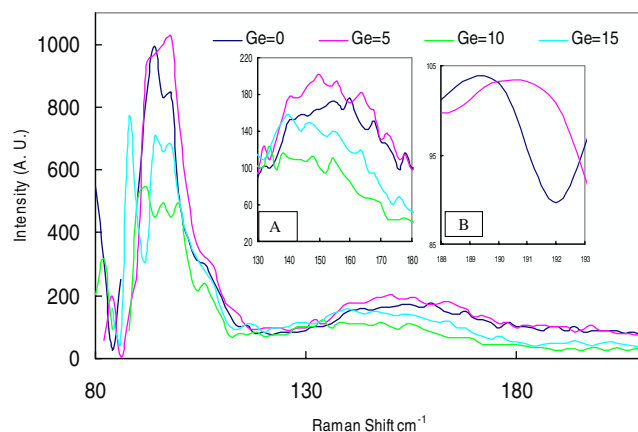


Figure 2. Raman spectra of $\text{Sb}_{65}\text{Se}_{35-x}\text{Ge}_x$ ($x = 0\text{--}20$ at.%) thin films.

$\text{Se}_2\text{Sb}\text{--SbSe}_2$ structural units [18], due to the excess amount of antimony and the Se deficiency (the parameter R is less than 1; see table 1). It is interesting to note that the 192 cm^{-1} (see inset (B)) band is present, albeit quite weakly, even in the Raman spectrum of $\text{Sb}_{65}\text{Se}_{30}\text{Ge}_5$. This result is indicative of violation of the chemical order and the presence of a small concentration of Sb–Sb homopolar bonds in the structure of this composition. No major change in the shape and position of the characteristic vibration bands with an increase in Ge content has been observed. Moreover, the lowest frequency band and the band at around 148 cm^{-1} have intensities that decrease with the progressive addition of Ge to 5 at.%, corresponding to GeSe_4 tetrahedra and SbSe_3 pyramids that are weakly coupled through two atomic –Se–Se bridging groups. This means that the two bands could be the combined effect of the bending modes of Sb–pyramidal units and/or Ge–tetrahedral units, and the addition of germanium to 5 at.% causes a reduction in the intensity of the bands. However, the intensity of these bands decreases when 5 at.% Ge is added to the binary system showing, that the introduction of germanium leads to a decrease in the number of homopolar Sb–Sb bonds and increases the number of heteropolar Ge–Se bonds. Moreover, in addition to the main bands that appear around $88\text{--}120$ and $130\text{--}180\text{ cm}^{-1}$, a very broad, low-intensity peak at around 168 cm^{-1} is also observed in $\text{Sb}_{65}\text{Se}_{25}\text{Ge}_{10}$ films. The band at 168 cm^{-1} is assigned to Sb–Sb vibrations in $\text{Se}_2\text{Sb}\text{--SbSe}_2$

Table 1. Values of the optical gap (E_g^{opt}), average coordination number (Z), parameter R and average heat of atomization for amorphous $\text{Sb}_{65}\text{Se}_{35-x}\text{Ge}_x$ thin films.

| Ge (at.%) | E_g^{opt} (eV) | Z | Parameter R | H_s | H_s/Z |
|-----------|-------------------------|------|---------------|-------|---------|
| 0 | 0.73 | 2.65 | 0.36 | 57.59 | 21.73 |
| 5 | 0.9 | 2.75 | 0.28 | 59.62 | 21.68 |
| 10 | 0.63 | 2.85 | 0.21 | 61.65 | 21.63 |
| 15 | 0.66 | 2.95 | 0.16 | 63.68 | 21.59 |
| 20 | 0.67 | 3.05 | 0.11 | 65.71 | 21.54 |

units [22]. At 15 at% Ge substitution, there are three bands that could be assumed to be GeSe_4 tetrahedral and SbSe_3 pyramidal structural units.

The most important points are the following.

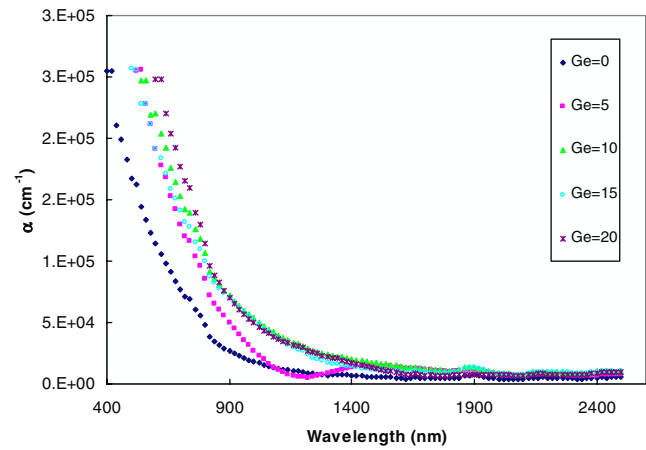
1. For the binary system ($\text{Sb}_{65}\text{Se}_{35}$ composition), the Raman spectrum indicates the presence of vibrational modes due to SbSe_3 structural units.
2. The vibration spectra must correspond primarily to vibrational modes involving Sb–Se bonds as Se–Se bonds would be highly unexpected in these Se-poor materials and stretching modes of Sb–Sb homopolar bonds are located at significantly higher frequencies.
3. The basic structural units of the ternary (Sb–Se–Ge) system are expected to be SbSe_3 pyramids with a threefold coordinated Sb atom at the apex and GeSe_4 tetrahedrons with Ge in the center which are weakly coupled through two atomic –Se–Se bridging groups.
4. The decrease in peak height and the upshift to higher values may be attributed to an increase in structural randomness [16].
5. By comparing the peak position and Raman intensity in the range of bond modes, it is derived that the changes occur non-monotonically with increasing Ge content.

The absorption coefficient was calculated [16] using the transmittance and reflectance readings that have been measured by the spectrophotometer,

$$\alpha = \frac{2.303}{d} \log_{10} \frac{(1-R)^2}{T}, \quad (1)$$

where T is the transmission, R the reflectance, α the absorption coefficient and d the film thickness. The variation of α as a function of wavelength (λ) for $\text{Sb}_{65}\text{Se}_{35-x}\text{Ge}_x$ thin films is shown in figure 3. It has been observed that the values of α decrease with an increase in wavelength for all films. An analysis of the absorption coefficient was carried out to obtain the optical energy gap E_g^{opt} . In many amorphous semiconductors, one can distinguish three different ranges.

- A high energy range ($\alpha \geq 10^4 \text{ cm}^{-1}$) corresponds to transition between extended states in both valence and conduction bands. In other words, the low-wavelength absorption data are related to interband transitions (i.e. excitation of an electron from the valence band to the conduction band) [26, 27].
- An intermediate region (α from 1 cm^{-1} or less up to 10^4 cm^{-1}) [28] or ($50 < \alpha < 5 \times 10^3 \text{ cm}^{-1}$) [29], where $\alpha(h\nu) = \alpha_0 \exp(h\nu/E_e)$; this is related to the tail of localized defect states at the band edges; E_e is the band tail width in semiconductors.

**Figure 3.** Plot of the absorption coefficient against wavelength for the as-prepared films.

- Below the exponential part of the absorption edge, an absorption tail is observed.

In the low-wavelength absorption region, the optical energy gap, E_g^{opt} , for Sb–Ge–Se films can be calculated from the following well-known quadratic equation [30–32], which is often called Tauc's law,

$$\alpha h\nu = \beta (h\nu - E_g^{\text{opt}})^r, \quad (2)$$

where $h\nu$ is the incident photon energy, β is a constant that depends on the electronic transition probability and the exponent r is a parameter that depends on the type of electronic transition responsible for the absorption. Values of $r = 2$ and $r = 0.5$ correspond, respectively, to allowed indirect and allowed direct optical transitions. Here, $r = 2$ offers the best fit for the optical absorption data of the investigated films. The plot of $(\alpha h\nu)^{0.5}$ versus $h\nu$ shown in figure 4 is almost linear and $\alpha \geq 10^4 \text{ cm}^{-1}$, supporting the allowed indirect [33, 34] band transition of the material. The band gap is determined near the absorption edge by extrapolating the straight portion of the plot of the energy axis. The calculated values of E_g^{opt} for the analyzed films are given in table 1. It is evident from the table that the optical band gap first increases for $x = 5$ and then decreases with an increase in germanium concentration. Optical absorption depends upon both the short-range order in the amorphous state and the defects associated with it. The change in the optical band gap in the present system may be partly due to the change in bonding from covalent to partially ionic and partly due to an increase in disorder [35–37]. The weak dependence of the energy gap on the Ge content suggests that the Ge is acting as an impurity center in the eutectic SbSe amorphous phase [33].

Optical parameters, namely the refractive index (n), extinction coefficient (k), real dielectric constants (ϵ') and the imaginary part of dielectric constant (ϵ'') for the examined films, were calculated as described elsewhere [38].

The energy band gap value is correlated with the physical parameters of glasses, such as the average coordination number (Z) and average heat of atomization (H_s), the latter being a measure of cohesive energy and representing the relative bond strength. The average coordination number Z of

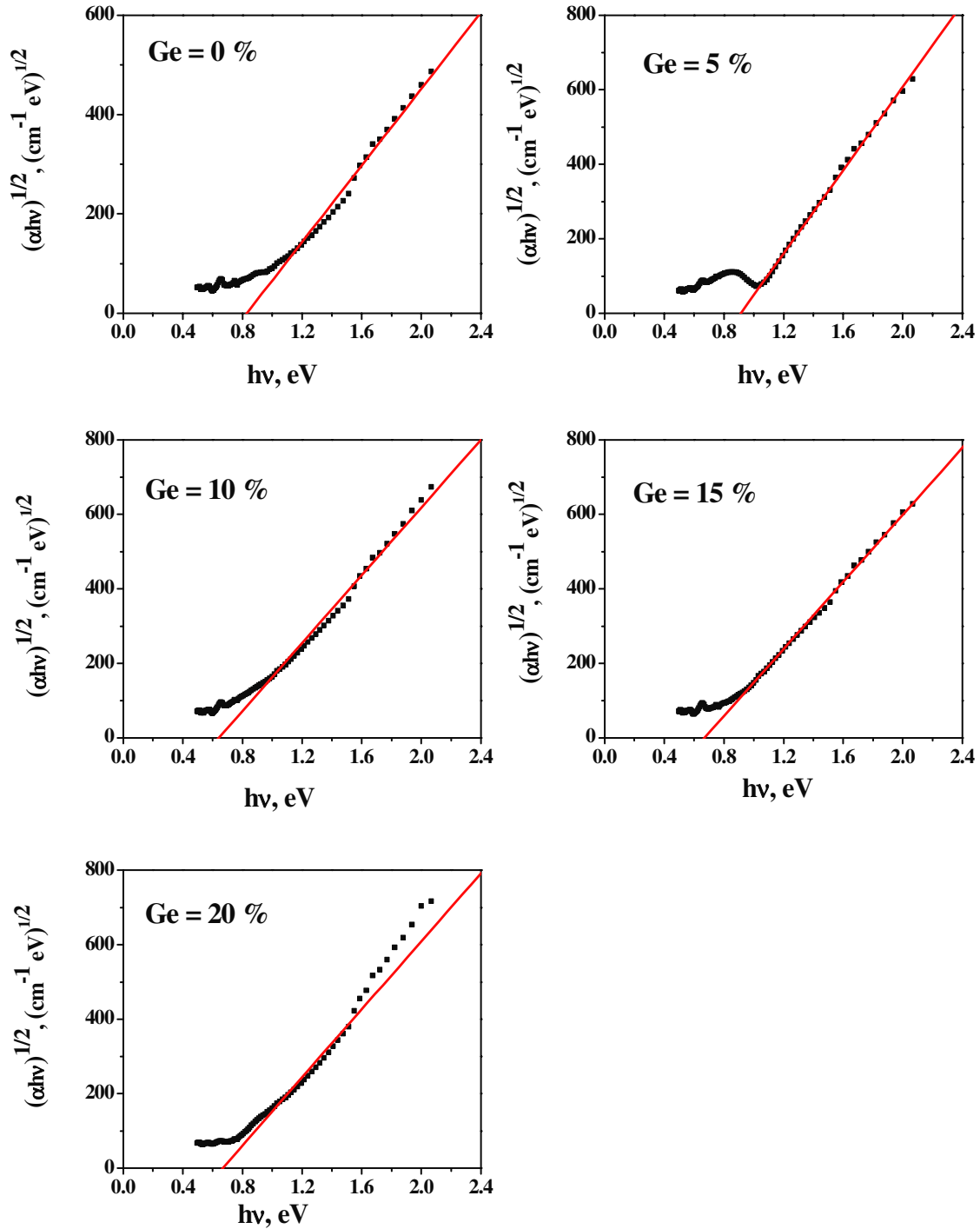


Figure 4. Plot of $(\alpha hv)^{0.5}$ versus $h\nu$ for $Sb_{65}Se_{35-x}Ge_x$ films.

a ternary $Ge_\alpha Sb_\beta Se_\gamma$ system is defined by the expression [39]

$$Z = \frac{4\alpha + 3\beta + 2\gamma}{\alpha + \beta + \gamma}, \quad (3)$$

where α , β and γ are the atomic percentages of Ge, Sb and Se, while 4, 3 and 2 are their coordination numbers. The coordination number Z characterizes the electronic properties of semiconducting materials and shows the bonding character in the nearest-neighbor region [40]. The average heat of atomization, H_s , for a ternary system $Ge_\alpha Sb_\beta Se_\gamma$ can be determined as [41]

$$H_s = (\alpha H_s^{Ge} + \beta H_s^{Sb} + \gamma H_s^{Se}) / (\alpha + \beta + \gamma), \quad (4)$$

where H_s is the heat of atomization of constituent atoms, and corresponds to the average nonpolar bond energy of the Ge–Ge, Sb–Sb and Se–Se chemical bonds [42]; α , β and γ are the atomic percentages of the corresponding elements. The calculated Z and H_s values, as well as their ratio, are summarized in table 1.

The variation in the optical energy gap (E_g^{opt}) with average coordination number (Z) is shown in figure 5. E_g^{opt} versus Z shows a clear change in slope at $x = 5$ ($Sb_{65}Se_{30}Ge_5$ composition) followed by a slight change above that composition. Therefore, the effect of germanium on SbSe appears to be limited to compositions with $x < 5$. This can be

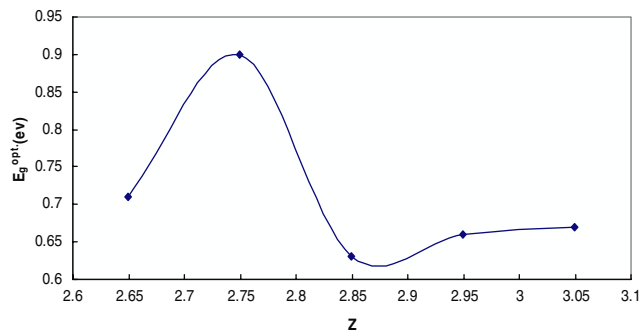


Figure 5. The variation of E_g^{opt} with Z for $\text{Sb}_{65}\text{Se}_{35-x}\text{Ge}_x$ thin films. The solid line is a guide to the eyes.

largely explained on the basis of the chemical ordered network model (CONM) proposed by Biecerano and Ovshinsky [43]. In CONM, the glass structure is assumed to be composed of cross-linked structural units of the stable chemical compounds (heteropolar bonds) of the system and excess, if any, of the elements (homopolar bonds). Due to the chemical ordering, features like the extremum, a change in the slope or a kink [44], occur for the various properties at the tie line composition or the chemical threshold of the system. For this composition, the system structure is made up of cross-linked pyramidal-like SbSe_3 and tetrahedral-like GeSe_4 structural units that consist of the energetically favored heteropolar bonds only. Heteropolar bonds thus have pre-eminence over homopolar bonds and bonds are formed in the sequences of decreasing bond energy until all the available valences of the atoms are saturated. Each constituent is coordinated by $8-N$ atoms, where N is the number of electrons in the outer shell and this is equivalent to neglecting the dangling bonds and other valence defects. As can be seen from figure 5, a maximum in the compositional dependence of E_g^{opt} is attained at $Z = 2.75$, which can be attributed to a change from a two-dimensional layered structure to a three-dimensional network arrangement due to cross-linking. This Z value lies in the region near Tanaka's threshold ($Z = 2.67$). According to the constraint theory [45], the investigated compositions are over-coordinated, stressed-rigid and with lower connectivity, as the values of Z are larger than 2.4. These observations indicate that the effects of chemical ordering are also present in this system along with the overall topological effects. In other words, the dependence of E_g^{opt} on Ge content and Z has been examined in light of topological and chemical ordered network models.

4. Conclusion

The structural and optical properties of $\text{Sb}_{65}\text{Se}_{35-x}\text{Ge}_x$ thin films have been studied. All the deposited thin films are amorphous in nature as confirmed by the XRD pattern. The results of the Raman spectroscopy experiments carried out on Sb–Se–Ge films show that the basic units, SbSe_3 pyramids and/or GeSe_4 tetrahedra persist in the glassy state for the whole range of the studied compositions. The optical band gap of the as-deposited films is allowed indirect transition and shows a weak dependence on Ge concentration, indicating that Ge acts as an impurity center in the amorphous eutectic SbSe phase.

The Z dependence of E_g^{opt} for Sb–Se–Ge thin films exhibit maxima at $Z = 2.75$, which can be understood as the realization of a chemical threshold in these films.

Acknowledgment

The authors acknowledge the Deanship of Scientific Research, Najran University, Najran, Saudi Arabia, for providing financial support (project no. NU 09/10).

References

- [1] Borg H J, van Shijndel M, Ripers J C N, Lankhorst M H R, Zhou G, Dekker M J, Ubbens I P D and Kuijper M 2001 *Japan. J. Appl. Phys.* **40** 1592
- [2] Khulbe P K, Hurst T, Horie M and Mansuripur M 2002 *Appl. Opt.* **41** 6220
- [3] Oomachi N, Ashida S, Nakamura N, Yuso K and Ichihara K 2002 *Japan. J. Appl. Phys.* **41** 1695
- [4] Lankhorst M H R, van Pieterse L, van Shijndel M, Jacobs B A J and Rijpers J C N 2003 *Japan. J. Appl. Phys.* **42** 863
- [5] Her Y-C and Hsu Y-S 2003 *Japan. J. Appl. Phys.* **42** 804
- [6] Kooia B J and De Hosson J Th M 2004 *J. Appl. Phys.* **95** 4714
- [7] Matsunaga T and Yamada N 2004 *Japan. J. Appl. Phys.* **43** 4704
- [8] van Pieterse L, Lankhorst M H R, van Schijndel M, Kuiper A E T and Roosen J H J 2005 *J. Appl. Phys.* **97** 083520
- [9] Lankhorst M H R, Ketelaars B W S M M and Wolters R A M 2005 *Nature Mater.* **4** 347
- [10] Saleh S A and Al-Hajry A 2010 *SPS5: 5th Meeting of the Saudi Physical Society, 'Physics and Energy Horizons' (Abha, Saudi Arabia, 25–27 Oct. 2010)*
- [11] Al-Ghamdi A A 2006 *Vacuum* **80** 400
- [12] Madan A and Shaw M P 1988 *The Physics and Applications of Amorphous Semiconductors* (Boston, MA: Academic)
- [13] Feltz A 1993 *Amorphous Inorganic Materials and Glasses* (Germany: VCH)
- [14] Kasap S O 2002 *Handbook of Imaging Materials* 2nd edn, ed A S Diamond and D S Weiss (New York: Marcel Dekker) p 329
- [15] Tanaka 2001 *Encyclopedia of Materials* (Oxford: Elsevier) p 1123
- [16] Mikla V I and Mikla V V 2010 *Metastable States in Amorphous Chalcogenide Semiconductors* (Berlin: Springer) pp 12, 16 and 18
- [17] Moharram A H 1998 *Appl. Phys. A* **66** 515
- [18] Sen S, Gjersing E L and Aitken B G 2010 *J. Non-Cryst. Solids* **356** 2083
- [19] Kumar P, Thangaraj R and Sathiaraj T S 2010 *J. Non-Cryst. Solids* **356** 1611
- [20] Petit L, Carlie N, Richardson K, Guo Y, Schulte A, Campbell B, Ferreira B and Martin S 2005 *J. Phys. Chem. Solids* **66** 1788
- [21] Kostadinova O and Yannopoulos S N 2009 *J. Non-Cryst. Solids* **355** 2040
- [22] Gutwirth J, Wagner T, Bezdzicka P, Vlcek M, Kasap S O and Frumar M 2007 *J. Non-Cryst. Solids* **353** 1431
- [23] Nguyen V Q, Sanghera J S, Freitas J A, Aggarwal I D and Lloyd I K 1999 *J. Non-Cryst. Solids* **248** 103
- [24] Sharma P, Rangra V S, Sharma P and Katyal S C 2009 *J. Alloys Compounds* **480** 934
- [25] Santos L F, Ganjoo A, Jain H and Almeida R M 2009 *J. Non-Cryst. Solids* **355** 1984
- [26] Fadel M, Fayek S A, Abo-Helal M O, Ibrahim M M and Shakra A M 2009 *J. Alloys Compounds* **485** 604
- [27] Mahdy I A, Domashevskaya E P, Seredin P V and Yatsenko O B 2011 *Opt. Laser Technol.* **43** 20
- [28] Kotkata M F, Kandil K M and Theye M L 1993 *J. Non-Cryst. Solids* **164–6** 1259

- [29] Tauc J 1974 *Amorphous and Liquid Semiconductors* (London: Plenum)
- [30] Khan S A, Khan Z H, El-Sebaï A A, Al-Marzouki F M and Al-Ghamdi A A 2010 *Physica B* **405** 3348
- [31] Al-Ghamdi A A and Khnan S A 2009 *Physica B* **404** 426
- [32] Khan S A and Al-Ghamdi A A 2009 *Mater. Lett.* **63** 1740
- [33] Prokhorov E, Mendoza-Galvan A, Gonzalez-Hernandez J and Chao B 2007 *J. Non-Cryst. Solids* **353** 1870
- [34] Abdel-Rahim M A, Hafiz M M, El-Nahass M M and Shamekh A M 2007 *Physica B* **387** 383
- [35] Khan Z H, Zulfeqar M and Hussian M 1997 *J. Mod. Opt.* **44** 55
- [36] Elliott S R and Steel A T 1987 *J. Phys. C: Solid State Phys.* **20** 4335
- [37] Ahmad M, Kumar P and Thangaraj R 2009 *Thin Solid Films* **517** 5965
- [38] Shokr E Kh and Wakkad M M 1992 *J. Mater. Sci.* **27** 1197–201
- [39] Yamaguchi N 1985 *Phil. Mag.* **51** 651
- [40] Ioffe A F and Regel A R 1960 *Prog. Semicond.* **4** 239
- [41] Pamukchieva V, Szekeres A, Todorova K, Svab E and Fabian M 2009 *Opt. Mater.* **32** 45
- [42] Pauling L 1960 *The Nature of the Chemical Bond* (Ithaca, NY: Cornell University Press)
- [43] Biecerano J and Ovshinsky S R 1985 *J. Non-Cryst. Sol.* **74** 75
- [44] Mahadevan S, Giridhar A and Singh A K 1988 *J. Non-Cryst. Solids* **103** 179
- [45] Phillips J C and Thorpe M F 1985 *Solid State Commun.* **53** 699